The phospholipase complex PAFAH Ib regulates the functional organization of the Golgi complex

Marie E. Bechler,[1] Anne M. Doody,[1] Esther Racoosin,[1] Lin Lin,[1] Kelvin H. Lee,[2] and William J. Brown[1]

[1]Department of Molecular Biology and Genetics and [2]Department of Biomedical Engineering, Cornell University, Ithaca, NY 14853

We report that platelet-activating factor acetylhydrolase (PAFAH) Ib, comprised of two phospholipase A_2 (PLA_2) subunits, α1 and α2, and a third subunit, the dynein regulator lissencephaly 1 (LIS1), mediates the structure and function of the Golgi complex. Both α1 and α2 partially localize on Golgi membranes, and purified catalytically active, but not inactive α1 and α2 induce Golgi membrane tubule formation in a reconstitution system. Overexpression of wild-type or mutant α1 or α2 revealed that both PLA_2 activity and LIS1 are important for maintaining Golgi structure. Knockdown of PAFAH Ib subunits fragments the Golgi complex, inhibits tubule-mediated reassembly of intact Golgi ribbons, and slows secretion of cargo. Our results demonstrate a cooperative interplay between the PLA_2 activity of α1 and α2 with LIS1 to facilitate the functional organization of the Golgi complex, thereby suggesting a model that links phospholipid remodeling and membrane tubulation to dynein-dependent transport.

Introduction

An unresolved feature of the Golgi complex is the role of membrane tubules in trafficking and maintenance of Golgi architecture (Bard and Malhotra, 2006; Pfeffer, 2007; De Matteis and Luini, 2008). Within the Golgi, membrane tubules are implicated in cis to trans cargo transport (Marsh et al., 2004; Trucco et al., 2004), retrograde trafficking to the ER (Lippincott-Schwartz et al., 1989; Saraste and Svensson, 1991), transport from the TGN to the cell surface and endosomes (Puertollano et al., 2001; Waguri et al., 2003; Bard and Malhotra, 2006; De Matteis and Luini, 2008), and in the assembly and maintenance of intact Golgi ribbons (de Figueiredo et al., 1998, 1999).

Pharmacological studies have shown cytoplasmic phospholipase A_2 (PLA_2) enzymes regulate the formation of Golgi membrane tubules that contribute to retrograde trafficking, and the assembly and maintenance of an intact Golgi ribbon in mammalian cells (de Figueiredo et al., 1998, 1999, 2000; Drecktrah and Brown, 1999; Polizotto et al., 1999; Brown et al., 2003). Here we identify platelet-activating factor acetylhydrolase (PAFAH) Ib as a cytoplasmic PLA_2 complex that regulates membrane tubule formation and organization and function of the Golgi complex. PAFAH Ib was originally purified based on its ability to hydrolyze the *sn-2* position acetyl group of the signal-transducing, phosphatidylcholine derivative, platelet-activating factor (PAF; Hattori et al., 1993, 1994a,b). PAFAH Ib consists of homo- or hetero-dimers of two closely related catalytic subunits, α1 (*Pafah1b3*) and α2 (*Pafah1b2*), and a non-catalytic dimer of β subunits (*Pafah1b1*; Ho et al., 1997; Arai et al., 2002; Tarricone et al., 2004). The β subunit is better known as LIS1, the causative agent of the fatal brain disorder Miller-Dieker lissencephaly (Kato and Dobyns, 2003). LIS1 is a highly conserved protein involved in dynein-mediated processes including nuclear and neuronal migration, centrosomal function, and mitotic spindle orientation (Kerjan and Gleeson, 2007; Vallee and Tsai, 2006). Although PAFAH Ib has been implicated in a variety of processes, including the regulation of PAF and LIS1 functions, its exact biological function is unclear, as $\alpha1^{-/-}/\alpha2^{-/-}$ double-knockout mice, although exhibiting defects

M.E. Bechler and A.M. Doody contributed equally to this paper.

Correspondence to William J. Brown: wjb5@cornell.edu

A.M. Doody's present address is Department of Biomedical Engineering, Cornell University, Ithaca, NY 14583.

K.H. Lee's present address is Biotechnology Institute, University of Delaware, Newark, DE 19711.

Abbreviations used in this paper: BBC, bovine brain cytosol; ERGIC, ER-Golgi intermediate compartment; LIS1, lissencephaly 1; PAF, platelet-activating factor; PAFAH, platelet-activating factor acetylhydrolase; PLA_2, phospholipase A_2; ssHRP, soluble secreted horseradish peroxidase; VSV-G, vesicular stomatitis virus G.

The Rockefeller University Press $30.00
J. Cell Biol. Vol. 190 No. 1 45–53
www.jcb.org/cgi/doi/10.1083/jcb.200908105

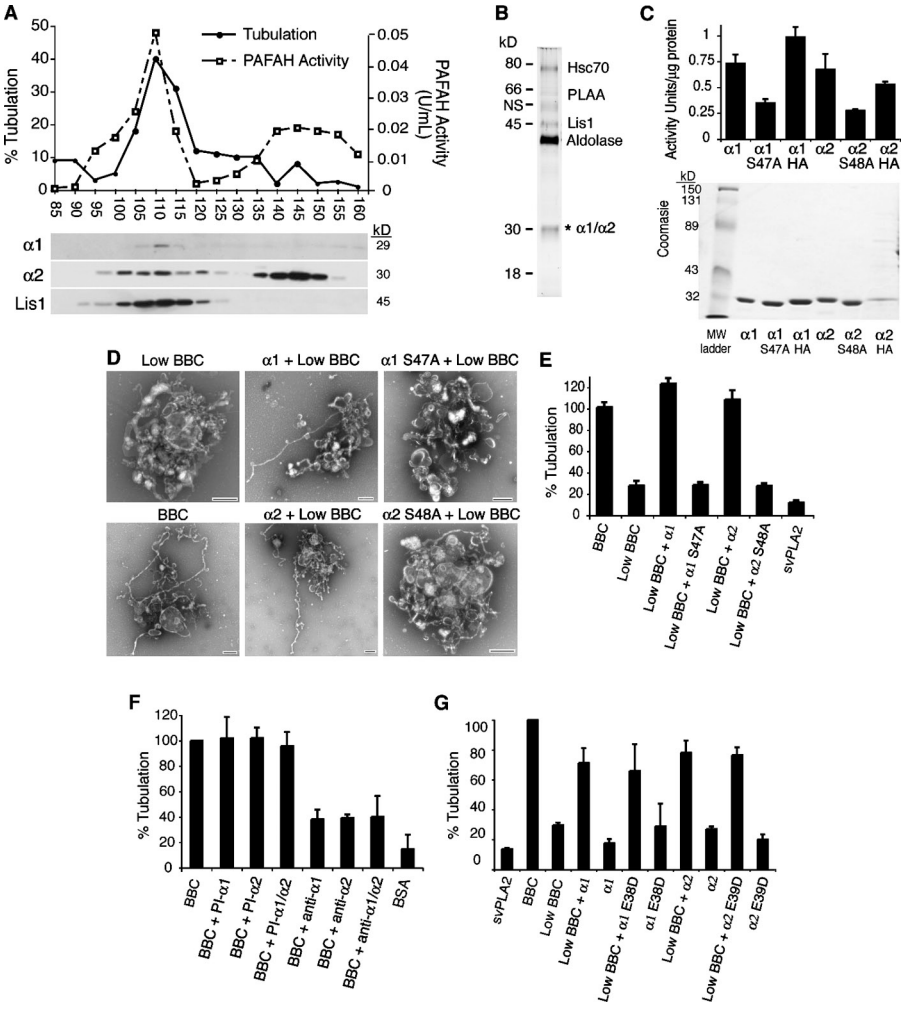

Figure 1. **PAFAH Ib catalytic subunits are cytosolic Golgi tubulation factors.** (A) Peak Golgi tubule–stimulating activity (determined by an in vitro reconstitution assay) cofractionates with PAFAH activity and PAFAH Ib subunits (Western blot) in final bovine brain cytosol (BBC) fractionation steps. (B) Silver stain of final fractions with the minimal components that stimulate Golgi tubules in vitro. The components identified by MALDI TOF-TOF and/or Western blot are labeled (NS = non specific). (C) Coomassie-stained gel and PAFAH activity of purified subunits. (D) EM of negative stain Golgi from in vitro tubulation reconstitution assays incubated with BBC and purified subunits as indicated. Bars, 500 nm. (E) Quantitation of tubulation assay using purified α1 and α2 subunits (7.5 μg/ml), with subthreshold BBC (low BBC, 0.25 mg/ml) compared with saturating BBC (1.5 mg/ml). svPLA$_2$ = snake venom PLA$_2$. Results are the percentage of control (BBC), $n = 4$; error bars = SD. (F) Anti-α1 and/or anti-α2 antibodies, but not preimmune IgG (PI-α1, PI-α2), inhibit cytosol-stimulated Golgi membrane tubules in vitro. BSA = bovine serum albumin. Results are percentage of control (BBC), $n = 4$; error bars = SD. (G) Quantitation of tubulation with purified wild-type or LIS1-binding defective α1 E38D and α2 E39D (7.5 μg/ml), in the presence or absence of low BBC. Results are percentage of control (BBC), $n = 3$; error bars = SEM.

in spermatogenesis, are otherwise normal (Koizumi et al., 2003; Yan et al., 2003).

Using multiple in vitro and in vivo approaches, we find that all three subunits of PAFAH Ib contribute to the structure of the mammalian Golgi complex, and the catalytic subunits independently contribute to secretion. Our results suggest a model whereby the PLA$_2$ activity of α1 and α2 remodel membrane phospholipids to form Golgi tubules, which are linked via LIS1 to dynein-mediated, microtubule transport.

Results and discussion

PAFAH Ib α1 and α2 are cytoplasmic membrane tubulation factors

Previous studies showed that a preparation of bovine brain cytosol (BBC) contains PLA$_2$ activity that stimulates Golgi membrane tubule formation in a cell-free system (de Figueiredo et al., 1999). Biochemical fractionation of BBC yielded a final gel filtration (GF) fraction highly enriched (~5,400 fold) in tubulation activity, with native molecular weight of 150–170 kD (Banta et al., 1995), and containing cofractionating proteins of ~80, 66, 45, 40, 30, and 18 kD (Fig. 1, A and B). MALDI TOF-TOF and Western blotting identified the 45-kD band as LIS1 and the 29–30-kD bands as α1 and α2 catalytic subunits of PAFAH Ib (Fig. 1 B). Other proteins identified in the GF fraction were Hsc70, PLA$_2$-activating protein (PLAA), and fructose bisphosphate aldolase. A variety of experiments showed that aldolase is a contaminant; the role of Hsc70 and PLAA in tubule formation, if any, remains to be determined.

To determine if PAFAH Ib is directly involved in membrane tubule formation, purified α1 or α2 was added to isolated Golgi complexes in vitro. Alpha subunits alone were unable to stimulate membrane tubules in the absence of BBC (Fig. 1 G). However, when α1 or α2 was mixed with subthreshold amounts of BBC, catalytically active α1 and α2 but not inactive enzymes with single amino acid changes in active site serines (α1 S47A; α2 S48A; Hattori et al., 1994b) significantly induced Golgi membrane tubule formation (Fig. 1, C–E). This cytosol requirement was not due to LIS1, because α1 or α2 mutants that do not bind to LIS1 (α1 E38D and α2 E39D; Yamaguchi et al., 2007) stimulated membrane tubules (Fig. 1 G). Consistent with these results, antibodies against α1 and α2 (but not preimmune antisera) inhibited BBC-dependent in vitro Golgi membrane tubulation (Fig. 1 F), whereas the addition of LIS1 antibodies had no effect (unpublished data). These results show that PAFAH Ib catalytic activity is required for stimulating membrane tubules from isolated Golgi complexes.

PAFAH Ib α1 and α2 partially localize to Golgi membranes and tubules

In mildly expressing cells, catalytically active HA-tagged α1 or α2 (Fig. 1 C) was found diffuse throughout the cytoplasm, in the nucleus, on punctate structures, and clearly on intracellular structures in the juxtanuclear region that colocalized with Golgi markers including Rab6-GFP (cis), GPP130 (cis), mannosidase II (ManII, *medial*), and mannose 6-phosphate receptors (M6PR, TGN; Fig. 2, A and B; Fig. S1 A; unpublished data). A similar distribution was seen by Caspi et al. (2003) in cells expressing GFP-α1. Catalytically inactive α1 S47A and α2 S48A, as well as α1 E38D and α2 E39D, were similarly localized (Fig. S1 A; unpublished data), indicating that catalytic activity and LIS1 binding are not required for α1 or α2 association with Golgi membranes. In addition to centrosomal and cytoplasmic localization, HA-tagged LIS1 was observed to surround the Golgi complex (Fig. 2, D and F), consistent with reports that a small fraction of LIS1 is membrane associated (Lam et al., 2010). PAFAH Ib α1 could also be found localized to membrane tubules (Fig. 2, E and G; Fig. S1 B). Consistent with the imaging results, we found that a fraction of both α1 and LIS1 cofractionated with Golgi membranes in sucrose gradients (Fig. 2 C).

PAFAH Ib α1 and α2 overexpression reveals a connection between PLA_2 activity and LIS1-mediated regulation of Golgi structure

Overexpression of α1 or α2 resulted in a fragmented or completely dispersed Golgi and TGN (Fig. 2, H and I; Fig. S2), which was more severe in α2-overexpressing cells (Fig. S2, A, C, and D). Changes in Golgi structure were not observed when cells overexpressed an unrelated cytoplasmic PLA_2, $iPLA_2\alpha$ (unpublished data). Overexpression of catalytically inactive α1 S47A or α2 S48A also caused the Golgi and TGN to become fragmented or diffuse (Fig. 2, H and I; Fig. S2). Overexpression of catalytically inactive α1 or α2 may produce a dominant-negative effect by forming poisonous dimers, competing with endogenous α1 and α2 for binding to membranes, and/or by titrating LIS1, thus inhibiting the ability of LIS1 to regulate dynein (Vallee and Tsai, 2006; Kerjan and Gleeson, 2007; Ding et al., 2009).

Microtubules and dynein-mediated centripetal positioning are required for the maintenance of an intact mammalian Golgi near the centrosome (Corthésy-Theulaz et al., 1992). To determine if overexpression of α1 and α2 affected Golgi structure by binding to and influencing LIS1 function, cells were transfected with the LIS1-binding mutants α1 E38D or α2 E39D. α2 E39D did disrupt the Golgi and TGN, albeit less severely than α2 wild-type or α2 S48A (Fig. 2 I; Fig. S2, D and E). In contrast to wild-type and catalytically inactive α1, overexpression of equivalent levels of α1 E38D did not significantly disrupt the Golgi or TGN (Fig. 2, H and I; Fig. S2, A–J), indicating that the Golgi disruption produced by α1 and α1 S47A are partially due to interactions with LIS1.

To determine if catalytic activity of α1 and α2 is also important for maintaining Golgi structure in vivo, independent of LIS1, cells were transfected with a double mutant that is both catalytically inactive and unable to bind LIS1 (α1 S47A/E38D; α2 S48A/E39D). These constructs also disrupted the Golgi and TGN (Fig. 2, H and I; Fig. S2, A–H).

The LIS1-binding mutant results suggest that catalytic activity is important, and that α subunits also compete for binding to LIS1 to regulate dynein-dependent Golgi structure, in agreement with previous reports (Ding et al., 2009). In addition, our results agree with Ding et al. (2009), who found that overexpression of α2 had a more dramatic effect on Golgi positioning. A role for LIS1 in Golgi structure has been suggested; $LIS1^{+/-}$ mouse embryonic fibroblasts had mild Golgi dispersal, and Cos-7 cells overexpressing LIS1 had more compact Golgi complexes (Smith et al., 2000).

Our results suggest a model whereby PAFAH Ib provides a link between the initiation of membrane tubule formation and the subsequent movement of these tubules along microtubules. PAFAH Ib α1 and α2, bound to LIS1, may initiate membrane curvature by intrinsic PLA_2 activity, thus forming membrane tubules. Subsequently, LIS1 may switch to a LIS1–Ndel1–dynein complex, facilitating the minus-end movement of membrane tubules along microtubules to the centrosome (Vallee and Tsai, 2006). This provides a mechanism to couple the formation of Golgi membrane tubules to dynein motors for the formation and maintenance of a centrally located, intact Golgi ribbon.

Loss of PAFAH Ib fragments the Golgi complex, inhibits tubule-mediated Golgi assembly, and reduces anterograde trafficking

To determine if PAFAH Ib α1 and α2 are required for Golgi structure and function, siRNA-mediated knockdown experiments were conducted. PAFAH Ib α1 and α2 can form catalytically active homo- and heterodimers (Manya et al., 1999). Therefore we used mixed siRNAs targeting both α1 and α2, reducing expression by 85.7 ± 3.3% and 81.8 ± 3.8% ($n = 7$ and 6; ± SEM), respectively, which did not affect levels of LIS1 (Fig. 3 A). As a consequence of α1 and α2 loss, the Golgi complex, ER-Golgi intermediate compartment (ERGIC), and the TGN became fragmented (Fig. 3, B–D; Fig. S3, A and B). Confocal microscopy revealed that fragmented Golgi puncta contained multiple cisternal markers, indicating that loss of α1 and α2 resulted in the formation of mini-stacks (Fig. 3 D; Fig. S3 C), which was confirmed by transmission EM (Fig. 3 E). Similar fragmentation was seen with knockdown of LIS1, which could be rescued by expressing RNAi-resistant HA-LIS1 (Fig. 3, F–H), similar to other recent studies (Lam et al., 2010).

Membrane tubule–mediated assembly and maintenance of an intact Golgi ribbon is inhibited by PLA_2 antagonists (de Figueiredo et al., 1999). To determine if knockdown of PAFAH Ib subunits similarly inhibits these tubules, we examined the reassembly of the Golgi during recovery from brefeldin A (BFA). After washout of BFA, the Golgi reassembles into separate mini-stacks that subsequently coalesce via membrane tubules into an intact ribbon (de Figueiredo et al., 1999). Knockdown of α1 and α2 or LIS1 had no apparent effect on BFA-stimulated retrograde movement of Golgi enzymes to the ER (unpublished data). Upon washout, the emergence of separate Golgi mini-stacks was unaffected by knockdown of PAFAH Ib subunits. In contrast, knockdown of α1 and α2 or LIS1 significantly inhibited subsequent coalescence into intact ribbons (Fig. 4, A–D),

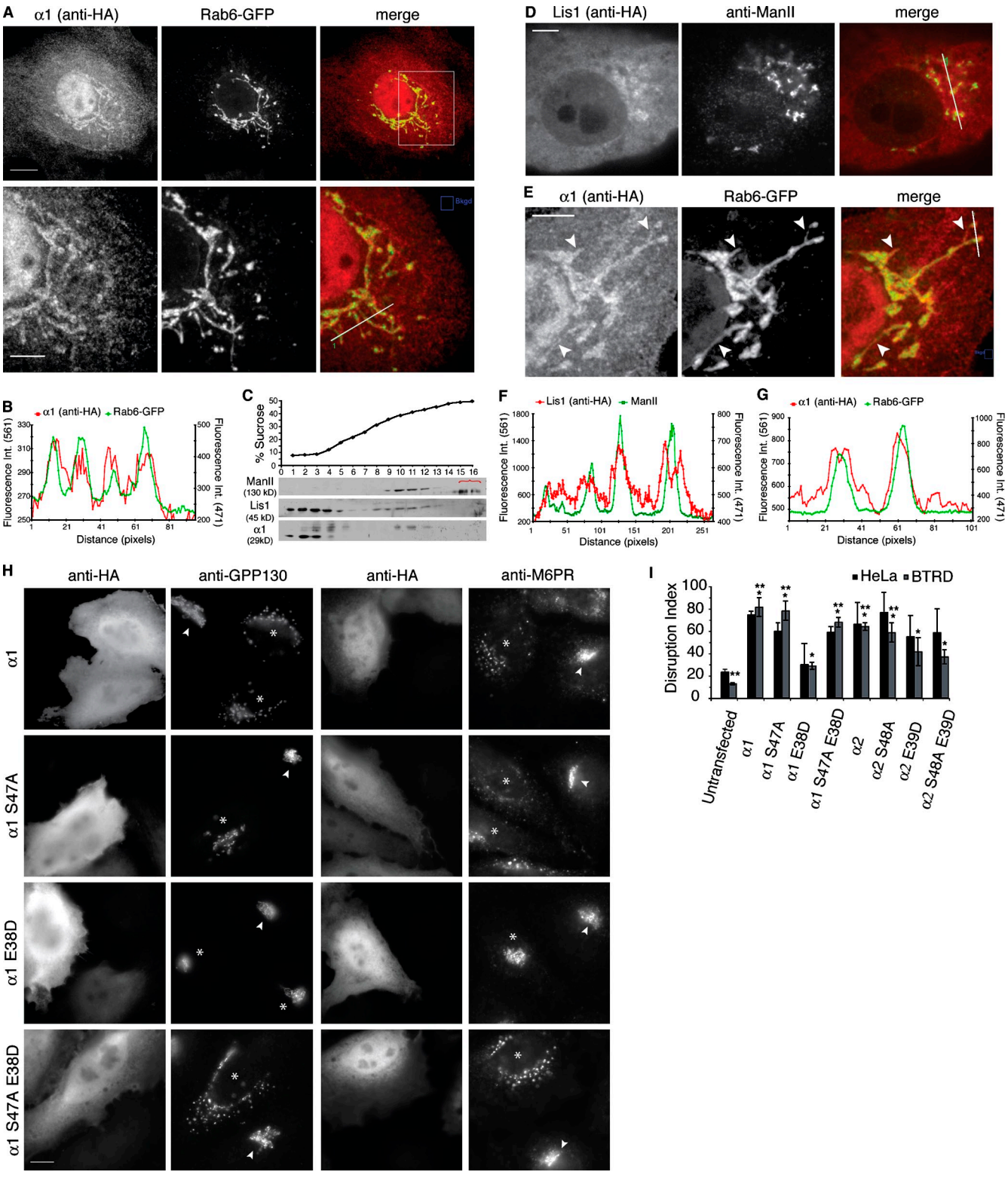

Figure 2. **PAFAH Ib partially localizes to Golgi membranes and overexpression of catalytic subunits perturbs Golgi and TGN structure.** (A) Confocal microscopy of cells mildly overexpressing α1 (HA tagged) and Rab6-GFP. Box indicates region in bottom panels. (B) Fluorescence intensity line plot of α1 and Rab6-GFP from bottom panel of A. (C) Western blot showing α1 and LIS1 cofractionate with Golgi (ManII) by sucrose-density cell fractionation. Bracket indicates nonspecific bands. (D) Confocal slice shows HA-LIS1 localizes around the Golgi (ManII). (E) α1 localizes to Golgi tubules. Arrowheads indicate colocalization with Rab6-GFP membrane tubules. (F) Line fluorescence intensity plot of LIS1 concentrated around Golgi complexes (from line in D). (G) Line fluorescence intensity of α1 on membrane tubules (from line in E). (H) HeLa cells transfected with the indicated α1 (HA tagged) and double labeled for HA and either a Golgi (GPP130) or TGN marker (M6PR). Overexpression of α1 wild type, α1 S47A (catalytic mutant), or α1 S47A/E38D (catalytic and LIS1-binding mutant) disrupted the structure of the Golgi and the TGN. Asterisks and arrowheads indicate transfected and untransfected cells, respectively. (I) Quantitation of HeLa and BTRD cells with disrupted Golgi structure in cells transfected as indicated. Weighted means shown, $n = 3$; error bars = SEM; *, $P < 0.05$ compared with untransfected cells; **, $P < 0.001$ compared with α1 E38D (Behrens-Welch test). Bars: (A, bottom, and E) 5 µm; (A, top, D, and H) 10 µm.

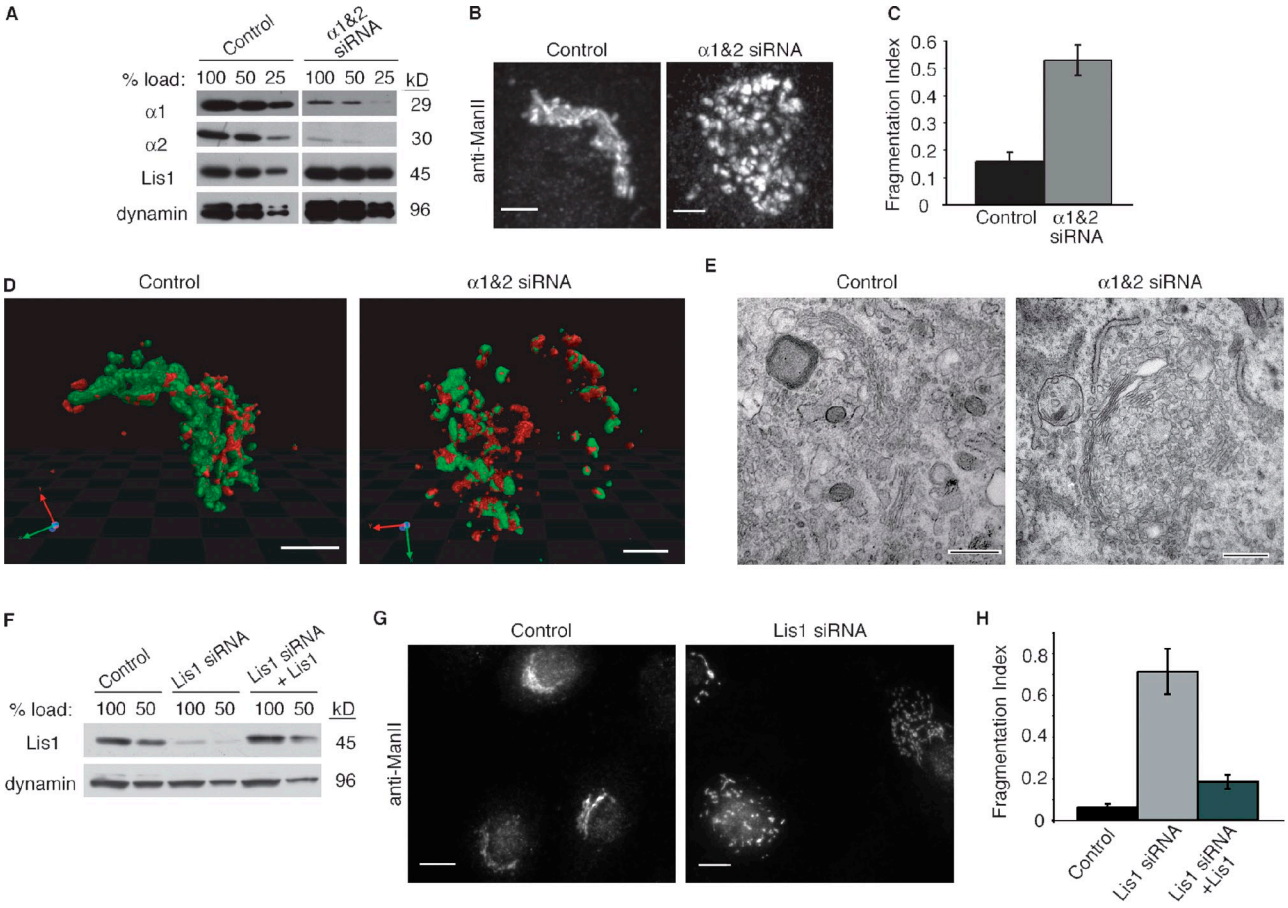

Figure 3. **PAFAH Ib subunits are important for maintaining an intact Golgi ribbon.** (A) Western blot of PAFAH Ib subunits in control and α1/α2 siRNA-treated (72 h) BTRD cells. (B) Confocal stack of the Golgi (ManII) in control and α1/α2 siRNA-transfected cells. (C) The fraction of cells with fragmented Golgi. $n = 7$; error bars = SEM; $P < 0.001$ by t test. (D) 3D reconstructions of Golgi from confocal z-series of control and α1/α2 siRNA-treated cells visualized with anti-ManII (*medial* marker, red) and GalT-GFP (trans marker, green). (E) Electron micrographs from control and α1/α2 siRNA knockdown cells. (F) Western blot 48 h after transfection of control BTRD cells, LIS1 siRNA-transfected cells, and LIS1 knockdown cells overexpressing RNAi-resistant HA-LIS1. (G) Wide-field fluorescence image of the Golgi (ManII) in control and LIS1 siRNA-transfected BTRD cells. (H) Fraction of cells with fragmented Golgi. $n = 3$; error bars = SEM. Bars: (B) 2 µm; (D and E) 500 nm; (G) 10 µm.

which could be rescued by expressing RNAi-resistant LIS1 (Fig. 4, C and D).Importantly, unlike α1 and α2 knockdown, LIS1 knockdown Golgi mini-stacks displayed numerous membrane tubules, which were no longer seen when all three subunits were knocked down (Fig. 4, E and F). These results are consistent with our in vitro and overexpression studies and further support the conclusion that the catalytic α1 and α2 subunits of PAFAH Ib are capable of inducing membrane tubules in vivo. The membrane tubules that form in LIS1 knockdown cells are dependent on α1 and α2, but directed movement for mini-stack coalescence is inhibited in the absence of LIS1-mediated dynein interactions.

In addition to reassembly of the Golgi complex, membrane tubules are implicated in export from the TGN and secretion (Bard and Malhotra, 2006; De Matteis and Luini, 2008). Using ts045VSV-G as a transmembrane cargo, we found that transport from the ER to the Golgi complex was unaffected in α1 and α2 knockdown cells (Fig. 5, A and B). In contrast, export of ts045VSV-G from the TGN to the cell surface was significantly slowed in α1 and α2 knockdown cells (Fig. 5, A, C, and D). VSV-G transport was unchanged with LIS1 knockdown (Fig. 5 F), suggesting α1 and α2 have LIS1-independent roles in TGN-to-plasma membrane trafficking. The reduced transport of VSV-G with α1 and α2 knockdown could be partially rescued by the reintroduction of equivalent levels of RNAi-resistant α1, but not RNAi-resistant α1 S47A, indicating that PLA_2 activity is important for regulating the transport of Golgi to plasma membrane cargo (Fig. 5 A, D; Fig. S2, I and J). Likewise, secretion of soluble cargo, ssHRP, was significantly inhibited in α1 and α2 knockdown cells (Fig. 5 E). Thus, loss of α1 and α2 may directly decrease TGN-to-plasma membrane tubulo-vesicular carriers (Bard and Malhotra, 2006; De Matteis and Luini, 2008).

Loss of α1 and α2 could also influence Golgi trafficking by affecting any number of components that require specific lipids for binding. Export from the TGN requires protein kinase D (PKD), which binds to membranes via diacylglycerol (Baron and Malhotra, 2002). A kinase-dead (KD) version of PKD, which inhibits TGN tubule fission (Bard and Malhotra, 2006), is a convenient marker for PKD association with the TGN. In α1 and α2 knockdown cells, PKD-KD-GFP underwent redistribution from the TGN to the cytoplasm and plasma membrane (Fig. S3 D). The structure and function of the Golgi and TGN is also dependent on COPI vesicles, AP-1 clathrin-coated vesicles, and microtubules;

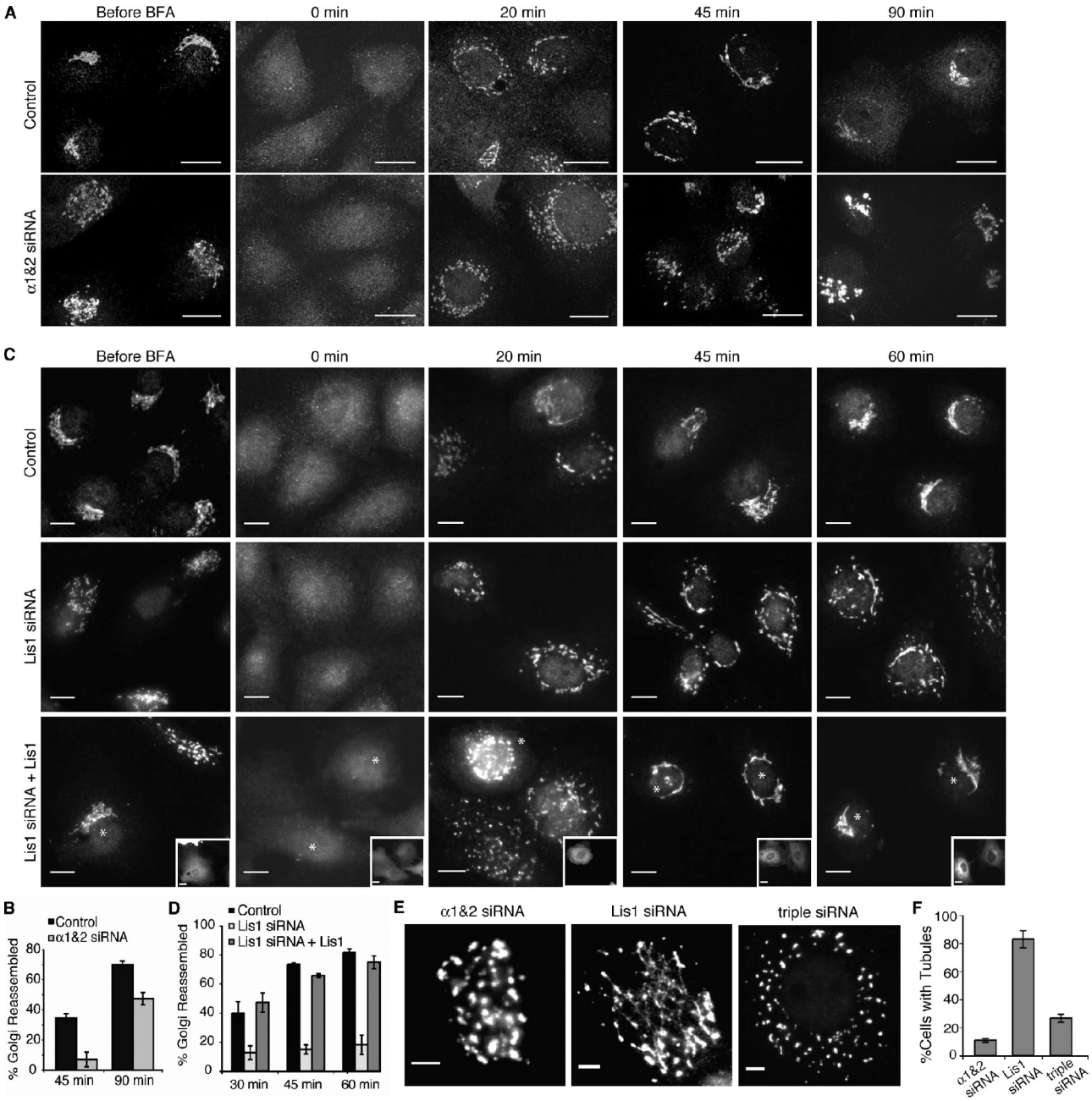

Figure 4. **Golgi ribbon reassembly is impaired in PAFAH Ib knockdown cells.** (A) Confocal images of the Golgi (anti-ManII) before BFA, after 20 min in BFA (0 min), and 20, 45, or 90 min after BFA washout in control or α1 and α2 siRNA-transfected cells. (B) Percentage of cells with reassembled Golgi ribbons after BFA washout. $n = 4$; error bars = SEM; at 90 min $P < 0.01$ by t test. (C) Wide-field fluorescence images of the Golgi (anti-ManII) before BFA treatment, and after 0, 20, 45, or 60 min of BFA washout. RNAi-resistant HA-LIS1 expression is shown in insets (anti-HA). (D) Percentage of cells with reassembled Golgi ribbons; $n = 3$; error bars = SEM. (E) Golgi mini-stacks (anti-ManII) after 30 min of BFA recovery for α1 and α2 siRNA or LIS1 siRNA, or α1/α2/LIS1 siRNA (triple)-treated BTRD cells. LIS1 knockdown cells show extensive membrane tubules, which are not seen in α1 and α2 or triple knockdown cells. (F) Percentage of cells with Golgi tubules after 30 min of BFA washout. Bars: (A and C) 10 µm; (E) 5 µm.

however, we found that knockdown had no discernable effect on β-COP, AP-1, or tubulin (Fig. S3, E and F). Similarly, the COPII vesicle component Sec31 was unaffected (Fig. S3 E). These results suggest that α1 and α2 contribute to phospholipid remodeling that is important for PKD association with the TGN.

It is becoming clear that Golgi structure and membrane trafficking require constant and complex phospholipid remodeling. In addition to PAFAH Ib, $cPLA_2\alpha$ has recently been shown to influence the Golgi by regulating tubule-mediated, cis-to-trans, inter-cisternal trafficking. Interestingly, loss of $cPLA_2\alpha$ can be compensated by PAFAH Ib α1 (San Pietro et al., 2009). $cPLA_2\alpha$ was also shown to regulate export from the TGN (Regan-Klapisz et al., 2009). Other recent studies found that another phospholipase, $iPLA_1\gamma$, contributes to tubule-mediated retrograde trafficking from the Golgi (Morikawa et al., 2009). Although the molecular mechanisms are unclear, continual phospholipid remodeling by PLA_1, PLA_2, and lysophosphatidyl acyltransferase enzymes, such as LPAAT3/AGPAT3

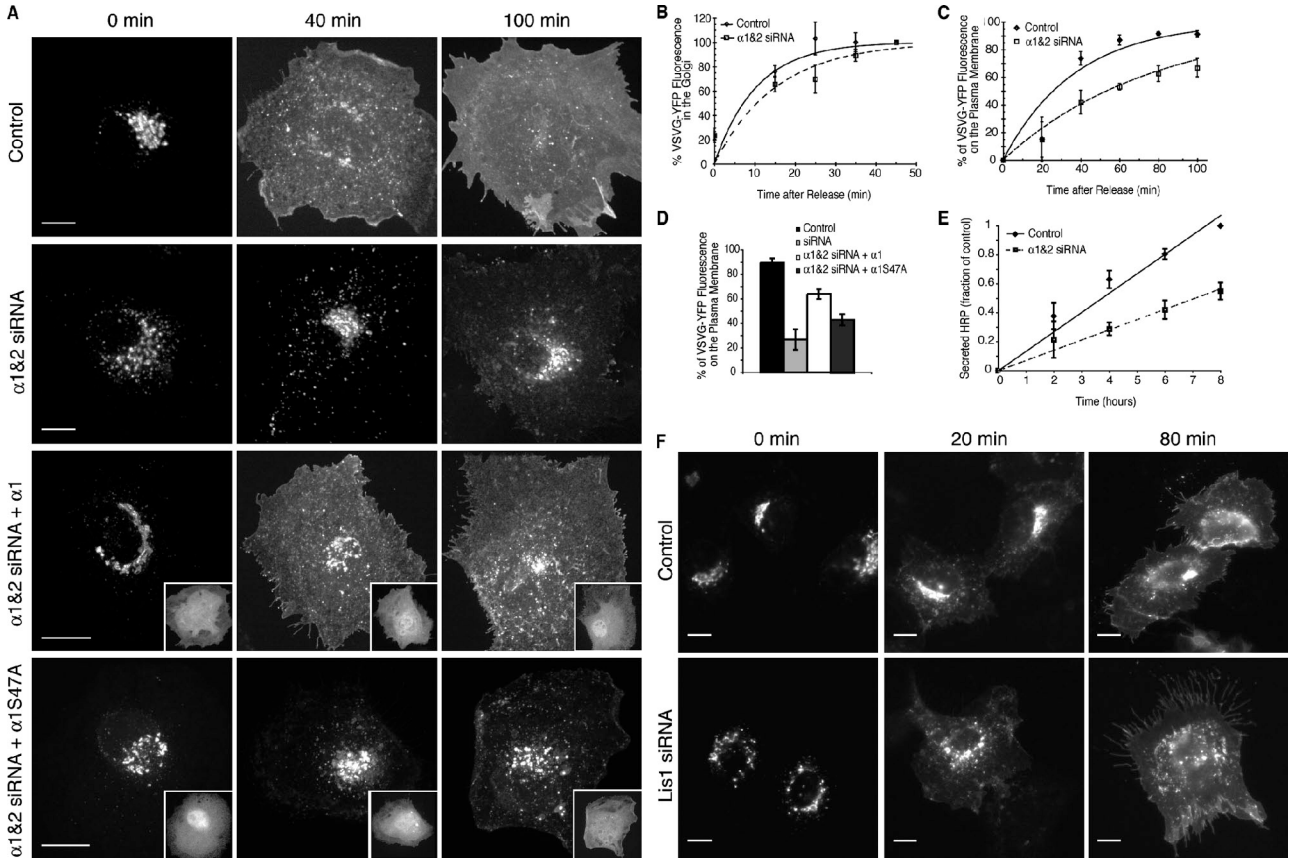

Figure 5. **PAFAH Ib α1 and α2 are important for the transport of both transmembrane and soluble cargo.** (A) Confocal stacks of ts045VSV-G-YFP after release from a 20°C TGN block in control, α1 and α2 siRNA-transfected, and either α1 and α2 siRNA + RNAi-resistant α1 or catalytic mutant α1 S47A-transfected BTRD cells. Insets show anti-HA, indicating α1 or α1 S47A-transfected cells. (B) Anterograde transport of ts045VSV-G from the ER to the Golgi. VSV-G-YFP fluorescence in the Golgi after release from a 40°C block to 20°C. Lines correspond to first order kinetic equations: control k = 0.10 ± 0.02 and siRNA k = 0.07 ± 0.02, ± SEM. Difference in kinetic constants was not statistically significant; $P < 0.25$ (*t* test). (C) Fluorescence intensity of post-TGN VSV-G-YFP fluorescence after release from 20°C. Lines correspond to first order kinetic equations, control k = 0.027 ± 0.005 and siRNA k = 0.013 ± 0.003, ± SEM; $P < 0.05$ (*t* test). (D) Fluorescence intensity of post-TGN VSV-G-YFP fluorescence after release from 20°C for control, α1 and α2 siRNA, and siRNA cells transfected with RNAi-resistant α1 or α1 S47A (catalytic mutant). (B–D) $n = 3–4$; error bars = SEM. (E) Secretion of ssHRP-Flag in control and α1 and α2 siRNA treated BTRD cells. Media HRP activity was measured and normalized to total HRP expression, expressed as a fraction of secreted HRP at 8 h in control cells. The rates of secretion were: control = 0.121 ± 0.003, α1 and α2 siRNA = 0.068 ± 0.008, ± SEM; $n = 8$; error bars = SEM. (F) VSV-G-YFP is transported from the Golgi to the plasma membrane in LIS1 siRNA-treated BTRD cells with rates similar to control cells, as seen by wide-field fluorescence. Bars, 10 µm.

(Schmidt and Brown, 2009), may be critical for regulating the availability of curvature-altering lipids such as lysophospholipids, phosphatidic acid, diacylglycerol, and/or for the recruitment of other membrane-trafficking proteins, such as PKD (Bankaitis, 2009).

Our results demonstrate a novel role for PAFAH Ib PLA_2 α subunits, which appear to be multi-functional, regulating PAF signaling, LIS1 function in dynein-mediated processes, and, as shown here, the formation of membrane tubules and the function of the Golgi complex. Our studies reveal a novel relationship of PAFAH Ib PLA_2 activity with dynein-dependent processes that are coupled by LIS1 to regulate Golgi structure. Additionally, our results show that α1 and α2 have a LIS1-independent role in export from the TGN.

Materials and methods

Materials

Sprague-Dawley male rats were from Charles River; BFA and cycloheximide from Enzo Life Sciences, Inc. Antibodies were as follows: rabbit anti-α1 and -α2 in initial studies (K. Inoue, University of Tokyo, Tokyo, Japan); guinea pig and rabbit anti-α1 and -α2 antibodies (characterized here); rabbit anti-bovine CI-M6PR (by us [Brown and Farquhar, 1987]); rabbit anti-dynamin (MC63; M. McNiven, Mayo Clinic, Rochester, MN); rabbit anti–human GPP130 (A. Linstedt, Carnegie Mellon University, Pittsburgh, PA); rabbit anti-ManII (K. Moremen, University of Georgia, Athens, GA); chicken anti-α2 (Abcam); mouse anti-LIS1 (Sigma-Aldrich); mouse anti-HA (Sigma-Aldrich and Covance); mouse anti–β-COP (BioMakor), mouse anti–α-tubulin (Sigma-Aldrich), rabbit anti–γ-adaptin (Santa Cruz Biotechnology, Inc.), rabbit anti-Sec31A (W. Balch, Scripps Research Institute, La Jolla, CA); fluorescent secondary antibodies (Jackson ImmunoResearch Laboratories, Inc. and Invitrogen); HRP-conjugated goat anti–chicken (Aves Laboratories), anti–guinea pig (Pocono Rabbit Farm and Laboratory), anti–rabbit (GE Healthcare), and anti-mouse (Invitrogen).

Preparation of plasmids

Bovine PAFAH Ib α1 and α2, pUC-P_L-cl-α1, and pUC-P_L-cl-α2 (Hattori et al., 1995) were gifts from Dr. Inoue. These were templates for α1-S47A and α2-S48A, which were made by PCR and ligation into pGEX6P1 (GE Healthcare) BamHI sites.

Tagging α1 and α2 on the N and C termini was problematic because such proteins were inactive. Although our polyclonal antibodies were useful for Western blots, we were unsuccessful in localizing endogenous α1 and α2 with many different polyclonal antibodies (made in rabbit, guinea pig,

chicken, and rat). Therefore, internally HA-tagged constructs were prepared by insertion on surface loops (α1 G165 and α2 P130, based on Ho et al., 1997) that would not interfere with dimer or LIS1 interactions. PCR products were ligated into EcoRI–SalI of pGEX6P-1.

Mammalian expression plasmids for α1-HA and α2-HA were constructed by ligation into EcoRI–XbaI-digested pEGFP-N1 (Takara Bio Inc.) to generate pEN1-α1-HA and pEN1-α2-HA. pEN1-α1-S47A-HA and pEN1-α2-S48A-HA were made by site-directed mutagenesis using QuikChange II (Agilent Technologies). LIS1-binding mutants (Yamaguchi et al., 2007) were generated by site-directed mutagenesis of pEN1-α1-HA, pEN1-α2-HA, pEN1-α1-S47A-HA, and pEN1-α2-S48A-HA. Two silent mutations in the dsRNA target sequence, using QuikChange II, were made to generate RNAi-resistant pEN1-α1-HA and pEN1-α1-S47A-HA.

pCMV-HA-LIS1 was a gift from Dr. R. Vallee (Columbia University, New York, NY). RNAi-resistant pCMV-HA-LIS1 was created by site-directed mutagenesis to generate two silent mutations in the dsRNA target sequence.

Protein purification

pGEX4T1-α1 and pGEX4T1-α2 were gifts of Dr. Z. Derewenda (University of Virginia, Charlottesville, VA). pGEX4T1-α1-E38D and pGEX4T1-α2-E39D were generated by site-directed mutagenesis. pGEX6P1-α1-S47A, pGEX6P1-α2-S48A, pGEX6P1-α1-HA, and pGEX6P1-α2-HA were prepared as described above. Proteins were purified and cleaved from GST using the GST-3C-Pro system or thrombin (Sigma-Aldrich) as described by GE Healthcare.

In vitro Golgi tubulation assay and mass spec protein identification

Reconstitution of Golgi membrane tubule formation and fractionation of BBC was as described previously (Banta et al., 1995). In brief, BBC was fractionated by a series of centrifugations to remove particulate material and several ammonium sulfate precipitations. A soluble fraction was subjected to a series of chromatographic separations including phenyl-sepharose, DE52 ion exchange, Affi-Gel blue, and finally gel filtration (GF) on Sephadex G100 that yielded a GF highly enriched in tubulation activity. BBC was combined with antibodies or purified proteins as described in the Results and discussion. GF fraction proteins were separated by 2D electrophoresis, excised, and digested with trypsin (Finehout and Lee, 2003). The peptide mixtures were analyzed using MALDI TOF-TOF on a 4700 Proteomics Analyzer (Applied Biosystems) as described previously (Hayduk et al., 2004). Using GPS Explorer v2.0 software (Applied Biosystems), MS and MSMS data were submitted as combined searches using the Mascot v1.9 search engine (Matrix Science) against an April 2004 download of the National Center for Biotechnology Information nonredundant sequence database (nr). Searches were limited to mammalian proteins and search hits. Only results at a GPS confidence interval >95% were accepted.

PAFAH activity assay

The PAFAH assay, using substrate 2-Thio PAF, was performed as described by the supplier (Cayman Chemical).

Cell culture, transfection, and RNAi

BTRD bovine testicular and HeLa cells were cultured in MEM (Mediatech, Inc.) with 10% BGS or NuSerum in a 37°C, 95% humidity, and 5% CO_2 incubator. Lipofectamine 2000 (Invitrogen) was used with modifications: DNA and reagent were reduced to a quarter. Experimentation was 24–48 h later. Double-stranded RNA targeting bovine α1 mRNA and bovine α2 mRNA were from Thermo Fisher Scientific: AGAAUGGAGAGCUGGAACAUU and GGAGAACUGGAGAAUAUUAUU, for α1 and α2, respectively. LIS1 dsRNA was from Thermo Fisher Scientific, sequence from Tsai et al. (2005). Control RNA was siGenome nontargeting siRNA #1 and #2 (Thermo Fisher Scientific). RNA was transfected on two consecutive days with Lipofectamine RNAiMax (Invitrogen) and 30 nM RNA. Experiments were 48 or 72 h after the initial RNA transfection.

Cell fractionation

BTRD cells were grown to confluency in six 24 × 24-cm dishes, washed with PBS (pH 7.4), harvested by scraping, and kept at 4°C or on ice. Cells were pelleted by low speed centrifugation and washed three times in homogenization buffer (0.25 mM sucrose, 1 mM EDTA, and 10 mM Tris, pH 7.4). Cells were homogenized in a Balch-Rothman apparatus, followed by a low speed centrifugation to obtain post-nuclear supernatant. The post-nuclear supernatant (~5 ml) was loaded on top of a linear 20–49% sucrose (10 mM Tris, pH 7.4) gradient and centrifuged in a SW28.1 rotor (Beckman Coulter) at 25,000 rpm for 2 h at 4°C with no brake. 1-ml fractions were collected from the cell fractionation gradient and prepared for SDS-PAGE and subsequent Western blotting. Fractions from a second parallel gradient were collected and used to measure sucrose concentration with an Abbe refractometer (Bausch & Lomb).

Fluorescence and electron microscopy

Cells were prepared as described previously (de Figueiredo et al., 1999, 2001). Either GFP- or YFP-tagged proteins or secondary antibodies conjugated to Alexa 488, DyLight 488, fluorescein isothiocyanate, tetramethylrhodamine isothiocyanate, or Cy5 were used. Coverslips were mounted with Vectashield (Vector Laboratories) mounting media and imaged at room temperature. Wide-field epifluorescence was with a microscope (Axioscope II; Carl Zeiss, Inc.) with 40x or 100x Plan-Apochromat NA1.4 oil objective lenses, a digital camera (Orca II; Hamamatsu Photonics), and Openlab software (PerkinElmer). Spinning disk confocal images were from a microscope (Eclipse TE2000-U; Nikon) with Plan-Apo 60x/NA1.4 or Plan-Apo100x/NA1.4 oil objectives, with an Ultraview LCI (PerkinElmer), a camera (1394 ORCA-ER; Hamamatsu Photonics), and Ultraview software (PerkinElmer). A microscope (DMI6000B; Leica) equipped with an oil 63x/NA1.4 objective, 3i Marianas spinning disk system, Photometrics HQII CCD camera, and 3i Slidebook 5.0 software was also used (Intelligent Imaging Innovations). For electron microscopy, FEI Morgagni 268 transmission EM was used.

VSV-G-YFP and ssHRP-Flag

ts045VSV-G-YFP pixel intensities of the juxtanuclear Golgi region and total cell were measured from confocal images using ImageJ (National Institutes of Health, Bethesda, MD), with appropriate background fluorescence subtraction (per area). Kinetic equations for ts045VSVG-YFP transport were fit by least squares nonlinear regression using Origin 3.5 software, based on first order kinetic equations (Hirschberg et al., 1998). For ssHRP-Flag measurements, media and lysate HRP activity was quantified by absorbance, using 3, 3′, 5, 5′-tetramethylbenzidine reagent (Sigma-Aldrich), and normalized to total HRP expression.

Image analysis and statistics

The Golgi disruption indices were by categorizing Golgi as diffuse, fragmented, or intact. For most experiments, ≥ 300 cells were counted for each condition, and each was repeated independently at least three times. The statistical significance between control and knockdown cells was with a two-tailed, unequal variance *t* test. The significance of overexpression phenotypes was by Behrens-Welch testing. Images and z-projections were cropped, brightness adjusted, or contrast adjusted using ImageJ, Photoshop CS3, or using 3i Slidebook 5.0 software. 3D reconstruction was done using Volocity software (PerkinElmer). Line intensity plots were done using 3i Slidebook 5.0 software (Intelligent Imaging Innovations).

Online supplemental material

Fig. S1 shows the localization of α1, α2, α2 S48A, or α1 S47A/E38D to multiple Golgi cisternae and TGN membrane tubules. Fig. S2 shows Golgi and TGN structure is disrupted upon overexpression of α1, α2, and various mutant α1 and α2 versions in HeLa and BTRD cell lines. Fig. S3 shows fragmentation of the ERGIC and TGN, and that the TGN is associated with Golgi mini-stacks with loss of α1 and α2 in siRNA knockdown experiments. Fig. S3 shows vesicle markers and microtubules are unaffected, whereas PKD-KD-GFP localization is changed upon α1 and α2 knockdown. Online supplemental material is available at http://www.jcb.org/cgi/content/full/jcb.200908105/DC1.

The authors would like to thank Dr. Z. Derewenda for plasmids encoding α1 and α2, and Drs. Junkin Aoki and Keizo Inoue for reagents used early in these studies. We also thank Leila Choe and Zsofia Franck for technical assistance with the mass spec analyses, Amy Antosh for help with electron microscopy, and Ina Chen for help with making the α1 and α2 LIS1-binding mutants.

This work was supported by National Institutes of Health grant DK51596 to W.J. Brown.

Submitted: 19 August 2009
Accepted: 14 June 2010

References

Arai, H., H. Koizumi, J. Aoki, and K. Inoue. 2002. Platelet-activating factor acetylhydrolase (PAF-AH). *J. Biochem.* 131:635–640.

Bankaitis, V.A. 2009. The Cirque du Soleil of Golgi membrane dynamics. *J. Cell Biol.* 186:169–171. doi:10.1083/jcb.200907008

Banta, M., R.S. Polizotto, S.A. Wood, P. de Figueiredo, and W.J. Brown. 1995. Characterization of a cytosolic activity that induces the formation of Golgi membrane tubules in a cell-free reconstitution system. *Biochemistry.* 34:13359–13366. doi:10.1021/bi00041a012

Bard, F., and V. Malhotra. 2006. The formation of TGN-to-plasma-membrane transport carriers. *Annu. Rev. Cell Dev. Biol.* 22:439–455. doi:10.1146/annurev.cellbio.21.012704.133126

Baron, C.L., and V. Malhotra. 2002. Role of diacylglycerol in PKD recruitment to the TGN and protein transport to the plasma membrane. *Science.* 295:325–328. doi:10.1126/science.1066759

Brown, W.J., and M.G. Farquhar. 1987. The distribution of 215-kilodalton mannose 6-phosphate receptors within cis (heavy) and trans (light) Golgi subfractions varies in different cell types. *Proc. Natl. Acad. Sci. USA.* 84:9001–9005. doi:10.1073/pnas.84.24.9001

Brown, W.J., K. Chambers, and A. Doody. 2003. Phospholipase A2 (PLA2) enzymes in membrane trafficking: mediators of membrane shape and function. *Traffic.* 4:214–221. doi:10.1034/j.1600-0854.2003.00078.x

Caspi, M., F.M. Coquelle, C. Koifman, T. Levy, H. Arai, J. Aoki, J.R. De Mey, and O. Reiner. 2003. LIS1 missense mutations: variable phenotypes result from unpredictable alterations in biochemical and cellular properties. *J. Biol. Chem.* 278:38740–38748. doi:10.1074/jbc.M301147200

Corthésy-Theulaz, I., A. Pauloin, and S.R. Pfeffer. 1992. Cytoplasmic dynein participates in the centrosomal localization of the Golgi complex. *J. Cell Biol.* 118:1333–1345. doi:10.1083/jcb.118.6.1333

de Figueiredo, P., D. Drecktrah, J.A. Katzenellenbogen, M. Strang, and W.J. Brown. 1998. Evidence that phospholipase A2 activity is required for Golgi complex and trans Golgi network membrane tubulation. *Proc. Natl. Acad. Sci. USA.* 95:8642–8647. doi:10.1073/pnas.95.15.8642

de Figueiredo, P., R.S. Polizotto, D. Drecktrah, and W.J. Brown. 1999. Membrane tubule-mediated reassembly and maintenance of the Golgi complex is disrupted by phospholipase A2 antagonists. *Mol. Biol. Cell.* 10:1763–1782.

de Figueiredo, P., D. Drecktrah, R.S. Polizotto, N.B. Cole, J. Lippincott-Schwartz, and W.J. Brown. 2000. Phospholipase A2 antagonists inhibit constitutive retrograde membrane traffic to the endoplasmic reticulum. *Traffic.* 1:504–511. doi:10.1034/j.1600-0854.2000.010608.x

de Figueiredo, P., A. Doody, R.S. Polizotto, D. Drecktrah, S. Wood, M. Banta, M.S. Strang, and W.J. Brown. 2001. Inhibition of transferrin recycling and endosome tubulation by phospholipase A2 antagonists. *J. Biol. Chem.* 276:47361–47370. doi:10.1074/jbc.M108508200

De Matteis, M.A., and A. Luini. 2008. Exiting the Golgi complex. *Nat. Rev. Mol. Cell Biol.* 9:273–284. doi:10.1038/nrm2378

Ding, C., X. Liang, L. Ma, X. Yuan, and X. Zhu. 2009. Opposing effects of Ndel1 and alpha1 or alpha2 on cytoplasmic dynein through competitive binding to Lis1. *J. Cell Sci.* 122:2820–2827. doi:10.1242/jcs.048777

Drecktrah, D., and W.J. Brown. 1999. Phospholipase A(2) antagonists inhibit nocodazole-induced Golgi ministack formation: evidence of an ER intermediate and constitutive cycling. *Mol. Biol. Cell.* 10:4021–4032.

Finehout, E.J., and K.H. Lee. 2003. Comparison of automated in-gel digest methods for femtomole level samples. *Electrophoresis.* 24:3508–3516. doi:10.1002/elps.200305615

Hattori, M., H. Arai, and K. Inoue. 1993. Purification and characterization of bovine brain platelet-activating factor acetylhydrolase. *J. Biol. Chem.* 268:18748–18753.

Hattori, M., H. Adachi, M. Tsujimoto, H. Arai, and K. Inoue. 1994a. Miller-Dieker lissencephaly gene encodes a subunit of brain platelet-activating factor acetylhydrolase [corrected]. *Nature.* 370:216–218. doi:10.1038/370216a0

Hattori, M., H. Adachi, M. Tsujimoto, H. Arai, and K. Inoue. 1994b. The catalytic subunit of bovine brain platelet-activating factor acetylhydrolase is a novel type of serine esterase. *J. Biol. Chem.* 269:23150–23155.

Hattori, M., H. Adachi, J. Aoki, M. Tsujimoto, H. Arai, and K. Inoue. 1995. Cloning and expression of a cDNA encoding the beta-subunit (30-kDa subunit) of bovine brain platelet-activating factor acetylhydrolase. *J. Biol. Chem.* 270:31345–31352. doi:10.1074/jbc.270.38.22308

Hayduk, E.J., L.H. Choe, and K.H. Lee. 2004. A two-dimensional electrophoresis map of Chinese hamster ovary cell proteins based on fluorescence staining. *Electrophoresis.* 25:2545–2556. doi:10.1002/elps.200406010

Hirschberg, K., C.M. Miller, J. Ellenberg, J.F. Presley, E.D. Siggia, R.D. Phair, and J. Lippincott-Schwartz. 1998. Kinetic analysis of secretory protein traffic and characterization of golgi to plasma membrane transport intermediates in living cells. *J. Cell Biol.* 143:1485–1503. doi:10.1083/jcb.143.6.1485

Ho, Y.S., L. Swenson, U. Derewenda, L. Serre, Y. Wei, Z. Dauter, M. Hattori, T. Adachi, J. Aoki, H. Arai, et al. 1997. Brain acetylhydrolase that inactivates platelet-activating factor is a G-protein-like trimer. *Nature.* 385:89–93. doi:10.1038/385089a0

Kato, M., and W.B. Dobyns. 2003. Lissencephaly and the molecular basis of neuronal migration. *Hum. Mol. Genet.* 12(Spec No 1, Spec No 1):R89–R96. doi:10.1093/hmg/ddg086

Kerjan, G., and J.G. Gleeson. 2007. Genetic mechanisms underlying abnormal neuronal migration in classical lissencephaly. *Trends Genet.* 23:623–630. doi:10.1016/j.tig.2007.09.003

Koizumi, H., N. Yamaguchi, M. Hattori, T.O. Ishikawa, J. Aoki, M.M. Taketo, K. Inoue, and H. Arai. 2003. Targeted disruption of intracellular type I platelet activating factor-acetylhydrolase catalytic subunits causes severe impairment in spermatogenesis. *J. Biol. Chem.* 278:12489–12494. doi:10.1074/jbc.M211836200

Lam, C., M.A. Vergnolle, L. Thorpe, P.G. Woodman, and V.J. Allan. 2010. Functional interplay between LIS1, NDE1 and NDEL1 in dynein-dependent organelle positioning. *J. Cell Sci.* 123:202–212. doi:10.1242/jcs.059337

Lippincott-Schwartz, J., L.C. Yuan, J.S. Bonifacino, and R.D. Klausner. 1989. Rapid redistribution of Golgi proteins into the ER in cells treated with brefeldin A: evidence for membrane cycling from Golgi to ER. *Cell.* 56:801–813. doi:10.1016/0092-8674(89)90685-5

Manya, H., J. Aoki, H. Kato, J. Ishii, S. Hino, H. Arai, and K. Inoue. 1999. Biochemical characterization of various catalytic complexes of the brain platelet-activating factor acetylhydrolase. *J. Biol. Chem.* 274:31827–31832. doi:10.1074/jbc.274.45.31827

Marsh, B.J., N. Volkmann, J.R. McIntosh, and K.E. Howell. 2004. Direct continuities between cisternae at different levels of the Golgi complex in glucose-stimulated mouse islet beta cells. *Proc. Natl. Acad. Sci. USA.* 101:5565–5570. doi:10.1073/pnas.0401242101

Morikawa, R.K., J. Aoki, F. Kano, M. Murata, A. Yamamoto, M. Tsujimoto, and H. Arai. 2009. Intracellular phospholipase A1gamma (iPLA1gamma) is a novel factor involved in coat protein complex I- and Rab6-independent retrograde transport between the endoplasmic reticulum and the Golgi complex. *J. Biol. Chem.* 284:26620–26630. doi:10.1074/jbc.M109.038869

Pfeffer, S.R. 2007. Unsolved mysteries in membrane traffic. *Annu. Rev. Biochem.* 76:629–645. doi:10.1146/annurev.biochem.76.061705.130002

Polizotto, R.S., P. de Figueiredo, and W.J. Brown. 1999. Stimulation of Golgi membrane tubulation and retrograde trafficking to the ER by phospholipase A(2) activating protein (PLAP) peptide. *J. Cell. Biochem.* 74:670–683. doi:10.1002/(SICI)1097-4644(19990915)74:4<670::AID-JCB16>3.0.CO;2-#

Puertollano, R., R.C. Aguilar, I. Gorshkova, R.J. Crouch, and J.S. Bonifacino. 2001. Sorting of mannose 6-phosphate receptors mediated by the GGAs. *Science.* 292:1712–1716. doi:10.1126/science.1060750

Regan-Klapisz, E., V. Krouwer, M. Langelaar-Makkinje, L. Nallan, M. Gelb, H. Gerritsen, A.J. Verkleij, and J.A. Post. 2009. Golgi-associated cPLA2alpha regulates endothelial cell-cell junction integrity by controlling the trafficking of transmembrane junction proteins. *Mol. Biol. Cell.* 20:4225–4234. doi:10.1091/mbc.E08-02-0210

San Pietro, E., M. Capestrano, E.V. Polishchuk, A. DiPentima, A. Trucco, P. Zizza, S. Mariggiò, T. Pulvirenti, M. Sallese, S. Tete, et al. 2009. Group IV phospholipase A(2)alpha controls the formation of inter-cisternal continuities involved in intra-Golgi transport. *PLoS Biol.* 7:e1000194. doi:10.1371/journal.pbio.1000194

Saraste, J., and K. Svensson. 1991. Distribution of the intermediate elements operating in ER to Golgi transport. *J. Cell Sci.* 100:415–430.

Schmidt, J.A., and W.J. Brown. 2009. Lysophosphatidic acid acyltransferase 3 regulates Golgi complex structure and function. *J. Cell Biol.* 186:211–218. doi:10.1083/jcb.200904147

Smith, D.S., M. Niethammer, R. Ayala, Y. Zhou, M.J. Gambello, A. Wynshaw-Boris, and L.H. Tsai. 2000. Regulation of cytoplasmic dynein behaviour and microtubule organization by mammalian Lis1. *Nat. Cell Biol.* 2:767–775. doi:10.1038/35041000

Tarricone, C., F. Perrina, S. Monzani, L. Massimiliano, M.H. Kim, Z.S. Derewenda, S. Knapp, L.H. Tsai, and A. Musacchio. 2004. Coupling PAF signaling to dynein regulation: structure of LIS1 in complex with PAF-acetylhydrolase. *Neuron.* 44:809–821.

Trucco, A., R.S. Polishchuk, O. Martella, A. Di Pentima, A. Fusella, D. Di Giandomenico, E. San Pietro, G.V. Beznoussenko, E.V. Polishchuk, M. Baldassarre, et al. 2004. Secretory traffic triggers the formation of tubular continuities across Golgi sub-compartments. *Nat. Cell Biol.* 6:1071–1081. doi:10.1038/ncb1180

Tsai, J.W., Y. Chen, A.R. Kriegstein, and R.B. Vallee. 2005. LIS1 RNA interference blocks neural stem cell division, morphogenesis, and motility at multiple stages. *J. Cell Biol.* 170:935–945. doi:10.1083/jcb.200505166

Vallee, R.B., and J.W. Tsai. 2006. The cellular roles of the lissencephaly gene LIS1, and what they tell us about brain development. *Genes Dev.* 20:1384–1393. doi:10.1101/gad.1417206

Waguri, S., F. Dewitte, R. Le Borgne, Y. Rouillé, Y. Uchiyama, J.F. Dubremetz, and B. Hoflack. 2003. Visualization of TGN to endosome trafficking through fluorescently labeled MPR and AP-1 in living cells. *Mol. Biol. Cell.* 14:142–155. doi:10.1091/mbc.E02-06-0338

Yamaguchi, N., H. Koizumi, J. Aoki, Y. Natori, K. Nishikawa, Y. Natori, Y. Takanezawa, and H. Arai. 2007. Type I platelet-activating factor acetylhydrolase catalytic subunits over-expression induces pleiomorphic nuclei and centrosome amplification. *Genes Cells.* 12:1153–1161. doi:10.1111/j.1365-2443.2007.01126.x

Yan, W., A.H. Assadi, A. Wynshaw-Boris, G. Eichele, M.M. Matzuk, and G.D. Clark. 2003. Previously uncharacterized roles of platelet-activating factor acetylhydrolase 1b complex in mouse spermatogenesis. *Proc. Natl. Acad. Sci. USA.* 100:7189–7194. doi:10.1073/pnas.1236145100